

## APPLIED CHEMISTRY

## A Study of the Catalytic Dehydrochlorination of 2-Chloropropane in Oxidizing Conditions

Chiara Pistarino, Elisabetta Finocchio, Giulia Romezzano, Fabrizio Brichese, Renzo Di Felice, and Guido Busca\*

*Dipartimento di Ingegneria Chimica e di Processo, Università di Genova, Pizzale J. F. Kennedy, I-16129 Genova, Italy*

Marco Baldi

*Dipartimento di Chimica, Università di Pavia, I-27100 Pavia, Italy*

The conversion of 2-chloropropane (2-CP) in the presence of oxygen has been investigated over a number of catalysts including alumina and alumina-supported copper chloride, manganese tungstate, mixed manganese–aluminum oxide, silica–alumina, and ZSM5 zeolite. Dehydrochlorination to propene + HCl is predominant, but other reactions such as oxychlorination to deeper chlorided compounds, cracking, oligomerization, and aromatization can occur. On silica–alumina, a selectivity to propene approaching 100% is found and very high conversion can be obtained above 400 K. Over this catalyst the reaction kinetics is found to be zero order in 2-CP with an activation energy near 14.5 kcal/mol. 2-CP converts definitely faster than 1-chloropropane. FT-IR spectroscopy shows that the molecular adsorption of 2-CP is fast and reversible at low temperature, while a nucleophilic substitution occurs to give strongly adsorbed 2-propoxide species starting from near 373 K. The elimination reaction of 2-propoxide to gas-phase propene occurs slowly just near 400 K. The desorption of HCl is also observed to be quite fast in this low-temperature range. FT-IR and kinetic data suggest that the rate-determining step is associated with the elimination reaction from 2-propoxides to propene occurring via an E1-type mechanism through a secondary carbenium ion.

## Introduction

The dehydrochlorination of chloroalkanes to olefins is a classical organic chemistry reaction occurring in the liquid phase in the presence of bases such as soda or calcium hydroxide with an elimination mechanism, either E1 or E2.<sup>1</sup> This reaction is carried out industrially, e.g., for the production of chloroprene from 3,4-dichloro-1-butene produced by partial chlorination of 1,3-butadiene<sup>2,3</sup> as well as for the production of vinylidene chloride from 1,1,2-trichloroethane.<sup>4,5</sup> The co-product of this stoichiometric reaction is NaCl so that both soda and chlorine are lost.

Alternatively, the elimination of HCl can be performed in the gas phase as a cracking, without any basic reactant, allowing the HCl product to be recovered. Industrially, this reaction is performed either thermally or catalytically.

The dehydrochlorination of 1,2-dichloroethane (EDC) is performed mostly as a thermal process to convert it into vinyl chloride (VCM), a still very largely used monomer. HCl is also recovered and recycled to the ethylene oxychlorination process to produce further EDC in the so-called “balanced” processes.<sup>6</sup> The endot-

hermic cracking elimination of EDC to VCM + HCl is performed industrially in cracking furnaces at 773–823 K and 2–3 MPa with a conversion of 50–60% and recycle of the unreacted EDC.<sup>6–8</sup> Catalytic cracking of EDC is also practiced industrially over silicates, metal-promoted aluminas, or zeolites,<sup>7,9</sup> but the advantage of working at lower temperatures does not apparently balance the drawback of needing catalyst regeneration. Recently, catalysis on poly(acrylonitrile)-based active carbon fiber catalysts<sup>10</sup> has been investigated for this reaction, although the catalyst lifetime was not long enough for practical application.

Dehydrochlorination of chlorinated linear paraffins is performed to produce linear olefins as intermediates to the synthesis of linear alkyl benzenesulfonate surfactants. This reaction can be carried out between 573 and 623 K in the presence of silica–alumina catalysts or on metal packings of reactor columns,<sup>11–13</sup> and HCl is recovered. In the open literature few studies are reported on gas-phase catalytic dehydrochlorination reactions, concerning dehydrochlorination of *tert*-butyl chloride over transition-metal chlorides<sup>14,15</sup> and dehydrochlorination of cyclohexyl chloride over silica-supported nickel catalysts in the presence of hydrogen<sup>16,17</sup> and of different compounds over alumina and silica–alumina.<sup>18</sup>

On the other hand, the dehydrochlorination of ethylene dichloride (EDC) has been recognized as an un-

\* Corresponding author. Fax: 39-010-3536028. E-mail: icibusca@csita.unige.it.

**Table 1. Catalysts**

catalyst	origin <sup>a</sup>	composition	surface area (m <sup>2</sup> /g)	XRD phase
CuCl <sub>2</sub> -Al <sub>2</sub> O <sub>3</sub>	impr.	9% Cu-Al <sub>2</sub> O <sub>3</sub> (w/w)	117	γ-Al <sub>2</sub> O <sub>3</sub>
Al <sub>2</sub> O <sub>3</sub>	STREM	Al <sub>2</sub> O <sub>3</sub>	225	γ-Al <sub>2</sub> O <sub>3</sub>
ZSM5	Zeolyst	Si:Al = 30:1	>400	ZSM5
SiO <sub>2</sub> -Al <sub>2</sub> O <sub>3</sub>	STREM	87% SiO <sub>2</sub> -13% Al <sub>2</sub> O <sub>3</sub>	330	amorphous
WO <sub>3</sub> -Al <sub>2</sub> O <sub>3</sub>	impr.	26.5% WO <sub>3</sub> -73.5% Al <sub>2</sub> O <sub>3</sub>	148	amorphous
MnO <sub>x</sub> -Al <sub>2</sub> O <sub>3</sub>	coprec.	atomic ratio Mn:Al = 1:1	106	α-Mn <sub>3</sub> O <sub>4</sub> -α-Mn <sub>2</sub> O <sub>3</sub> -γ-Al <sub>2</sub> O <sub>3</sub>
W-Mn-Al <sub>2</sub> O <sub>3</sub>	impr.	Mn <sub>3</sub> O <sub>4</sub> :WO <sub>3</sub> :Al <sub>2</sub> O <sub>3</sub> = 10.5:30.5:59 (w/w)	144	MnWO <sub>4</sub> , γ-Al <sub>2</sub> O <sub>3</sub>

<sup>a</sup> impr. = impregnation. coprec. = coprecipitation.

wanted byreaction occurring on the support surface of CuCl<sub>2</sub>-Al<sub>2</sub>O<sub>3</sub>-based catalysts upon ethylene oxychlorination, giving rise to VCM as a byproduct.<sup>19,20</sup> The formation of VCM in the oxychlorination reactor is very negative because it can be further oxychlorinated to ethyl trichloride and further transformed. These byreactions tend to lower the selectivity to EDC in the oxychlorination process. The alumina-catalyzed dehydrochlorination of ethyl chloride has been investigated in the frame of these studies as a test reaction.<sup>19</sup>

Finally, the dehydrochlorination can be a process allowing the (at least partial) dechlorination and recovery of chlorine from chlorine-containing organic wastes previous to their incineration. It is, in fact, well-known that the incineration of such wastes [chlorinated solvents to be disposed and poly(vinyl chloride) (PVC) itself] is environmentally dangerous because of the easy production of poly(chlorodibenzodioxins) and furans (PCDDs and PCDFs) and is, accordingly, limited by law. For these reasons we undertake a study of the catalytic dehydrochlorination of 2-chloropropane taken as an example of a weakly chlorided volatile organic compound.

## Experimental Section

Some data on the catalysts investigated are reported in Table 1. Gases were from SIAD (Milano, Italy), while 1- and 2-chloropropane (1-CP and 2-CP) were from Aldrich. Catalytic tests were carried out at atmospheric pressure in a continuous fixed-bed tubular glass flow reactor. A total of 0.1–0.4 g of catalyst was loaded in the form of a fine powder (mesh 60–70) mechanically mixed with a quartz powder. The total gas flow was in the range 345–370 mL/min, and the feed composition changed from 0.1% to 4% of chloropropane and 20% of oxygen, balance helium. The reactants and the reaction products were analyzed on line using a gas chromatograph (GC; HP 5890) equipped with a HP PLOT Q column connected to thermal conductivity and flame ionization detectors. A methanizer allowed the analysis of CO and CO<sub>2</sub>. GC-MS analysis of the products has been performed using a HP GCD1800D instrument with an HP-VOC column.

To analyze HCl and Cl<sub>2</sub>, the effluents were contacted with a NaOH–water solution. Chloride and hypochlorite anions have been analyzed and quantified by means of ionic chromatography. Actually, hypochlorite anions were never detected. According to this analysis, HCl only is produced and always nearly fulfilled the chlorine balance, if organic chlorided compounds analyzed by GC and GC-MS are taken into account. So, hereinafter only conversion and selectivities based on carbon-containing compounds are considered.

The results will be presented as conversions (*C*) and selectivities (*S*), both calculated on molar bases. The experimental error was estimated to not exceed 5%.

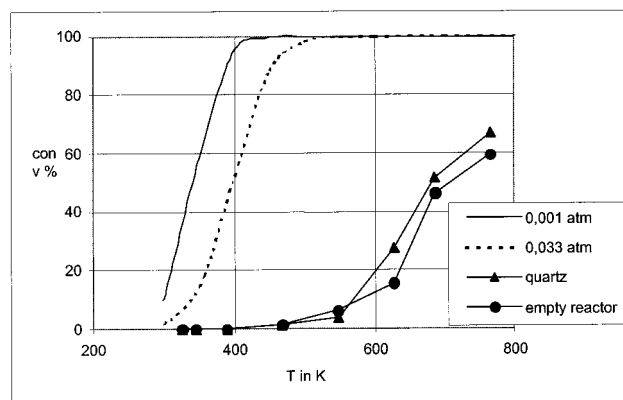


**Figure 1.** Theoretical thermodynamic conversion (*C*) of 2-CP with starting  $p_{2-CP} = 0.001$  and 0.033 atm and experimental conversions measured for the empty reactor and for the reactor containing a bed of quartz powder only.

FT-IR spectra have been recorded with a Nicolet Magna 750 instrument connected to a conventional gas-manipulation apparatus. Adsorption experiments have been carried out over pure catalyst powders pressed into self-supporting disks of the approximate weights of 20 mg.

## Results and Discussion

**1. Reaction Thermodynamics and Behavior in the Empty Reactor.** According to thermodynamic literature data,<sup>21</sup> the conversion of 2-CP to propene and HCl



is associated with the following standard free energy of reaction:

$$\Delta G_{298,r}^\circ = 28.8 \text{ kJ/mol} \quad (2)$$

This is an endothermic equilibrium reaction favored by increasing temperature and by decreasing pressure. In Figure 1 we have plotted the theoretical thermodynamic conversions calculated at the minimum and maximum reactant partial pressures used hereinafter, in the temperature range of interest in the present study, taking into account the effect of temperature on the specific heats of the compounds involved. It is evident that, at room temperature the reaction is thermodynamically unfavored, near 400 K the equilibrium shifts toward the products, and theoretical conversion approaches totality at higher temperature. The curves also show the adverse effect of increasing pressure on this equilibrium, significant in the region 350–450 K.

Experimental conversions in the empty reactor and in the reactor filled only with quartz particles by using

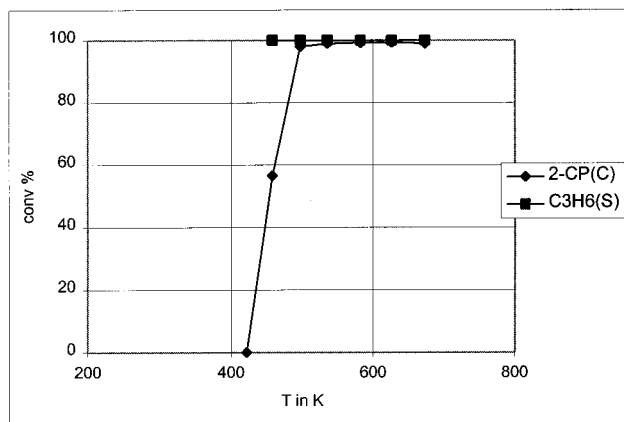


**Figure 2.** Conversion (C) of 2-CP and propene selectivity over a  $\gamma$ - $\text{Al}_2\text{O}_3$  catalyst with  $p_{2\text{-CP}} = 0.001$  atm and oxygen excess.

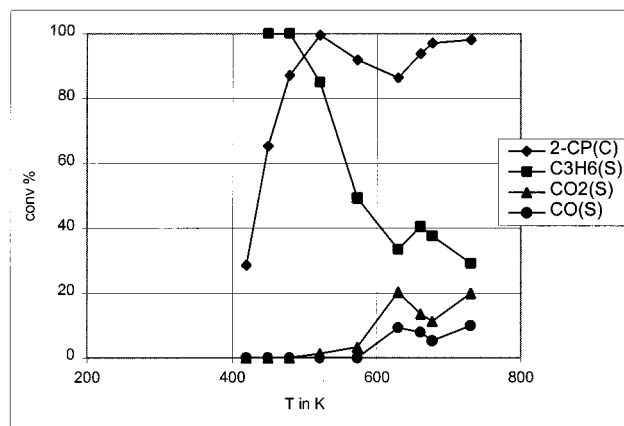


**Figure 3.** Conversion (C) of 2-CP and product selectivity (S) over a  $\text{CuCl}_2$ - $\gamma$ - $\text{Al}_2\text{O}_3$  catalyst with  $p_{2\text{-CP}} = 0.001$  atm and oxygen excess (total flow rate 350 mL/min).

reactant flow conditions similar to those used in the further experiments (2-CP partial pressure 0.025 atm) are also reported in Figure 1. The residence time in the overall heated reactor in these conditions is 1.7 min. Conversion starts to be detectable at 550 K and is nearly 30% at 630 K in the presence of quartz. Thus, the conversion in the range 300–650 K is limited by kinetics. The actual conversions we will observe upon our experiments in the presence of the catalyst beds in the temperature range 350–550 K reflect entirely the catalytic activity of the bed materials.

**2. Flow Reactor Experiments. 2.1. Conversion over Alumina and Alumina-Based Catalysts.** Over pure alumina by feeding 0.001 atm of 2-CP in helium–oxygen, the conversion starts to be detectable just above 400 K and approaches 100% at 480 K (Figure 2), while selectivity to propene is total, at least up to 750 K. Mass spectra analysis at 673 K shows chloropropenes as the main byproducts, in trace amounts.

Over  $\text{CuCl}_2$ -alumina catalyst, 2-CP conversion also starts near 400 K, with conversion rising to very high values above 500 K (Figure 3), although the conversion curve follows an irregular trend. Propene is the only reaction product at incomplete conversion, while at increasing temperatures (e.g., 600 K) selectivity to propene decreases to 30%. In the same temperature range, CO and  $\text{CO}_2$  formation become noticeable, even if their selectivities together do not attain 30%. Thus, we have evidence of an oxidizing activity, due to the presence of Cu ions at the surface. Several other

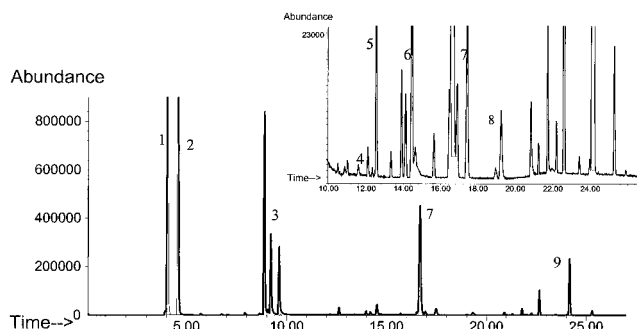


**Figure 4.** GC-MS analysis of the products arising from 2-CP conversion over a  $\text{CuCl}_2$ - $\gamma$ - $\text{Al}_2\text{O}_3$  catalyst at 673 K and with the same flow conditions as Figure 2. Some peak attributions: (1)  $\text{O}_2$ - $\text{CO}_x$ , (2)  $\text{C}_3\text{H}_6$ , (3)  $\text{C}_3\text{H}_5\text{Cl}$  isomers, (4) ether (diisopropyl ether), (5)  $\text{CHCl}_3$ , (6) dichloropropenes (i.e., 1,1-dichloropropene), (7) 1,2-dichloropropane, (8)  $\text{C}_3\text{H}_4\text{Cl}_2$  isomers (likely 1,3-dichloropropenes), (9) trichlorinated (likely trichloroethane).

byproducts have been detected with the help of mass spectrometry in the temperature range 500–670 K. In particular, we had evidence of oxychlorination reactivity. The formation of several chlorinated isomers of propene (i.e., both allylic and vinylic Cl-containing compounds) is observed at 520 K. 1-CP is also present. It is possible to detect also higher retention time molecules, such as polychlorinated compounds (1,2-dichloropropane), cracking products (polychlorinated  $\text{C}_1$ 's), and oxygenate compounds (esters and anhydrides), indicating a complex reaction chemistry. However, the main byproduct is 1,2-dichloropropane, likely resulting from the oxychlorination of propene. At increasing temperature the product distribution becomes even more complex and byproduct formation is relevant, affecting significantly the selectivity to propene. At 670 K (Figure 4) polychlorination and cracking processes give rise to the following detected compounds: 1- and 3-chloropropene, chlorinated  $\text{C}_1$  and  $\text{C}_2$  (e.g., chloroform and chloroethane), dichloropropenes, oxygenate compounds (e.g., isopropyl ether in traces), chlorinated organic acid or esters, and other polychlorinated compounds. It is worth noting that increasing temperatures favor the formation of polychlorinated compounds and unsaturated chlorinated compounds, while the intensity of the GC peak due to 1,2-dichloropropane does not change. Thus, over this catalyst we can observe the reactivity due to the acidic support, i.e., dehydrochlorination and cracking, and the oxidizing oxychlorinating effect of the  $\text{CuCl}_2$  phase.

Over the  $\text{W-Al}_2\text{O}_3$  catalyst (Figure 5 A) 2-CP conversion is already detectable below 400 K and is above 85% at 450 K, reaching nearly 100% at 750 K, while selectivity to propene is near 90% at the highest conversions. On a Mn–alumina catalyst (coprecipitated, Figure 5B), the conversion also reaches almost 100% near 500 K and the selectivity to propene is above 90%. On the Mn-doped  $\text{W-Al}_2\text{O}_3$  catalyst (Figure 5C), the 2-CP conversion activity is a little lower (100% at 510 K). On the other hand, selectivity to propene is not higher than 50% at the total 2-CP conversion.  $\text{CO}_2$  has been detected in traces, but no CO is formed. Again, the low selectivity to propene is due to the formation of polychlorinated byproducts detectable by GC-MS.

These data show that pure alumina is a better catalyst than the doped aluminas we investigated, according to the highest selectivity obtained (in the case of these low-pressure experiments) to the desired products propene + HCl.

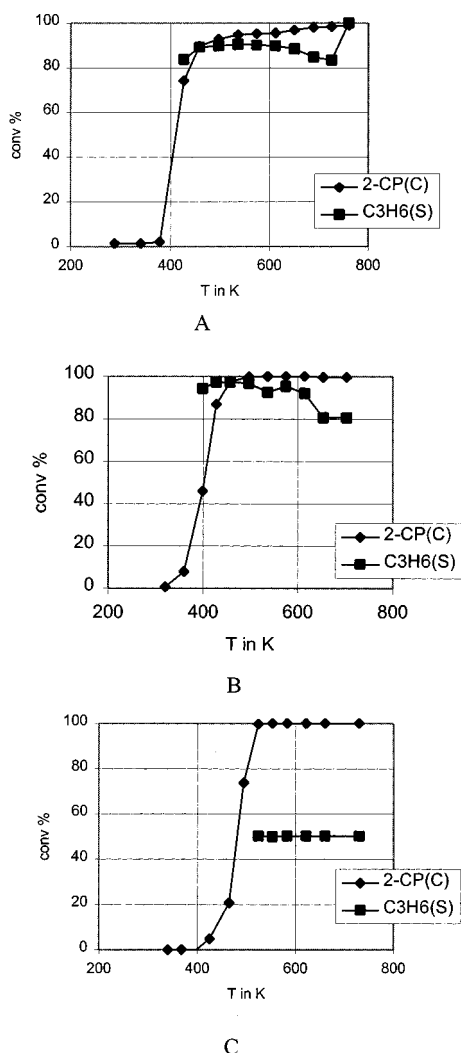


**Figure 5.** Conversion (C) of 2-CP and product selectivity (S) over  $\text{WO}_3\text{-}\gamma\text{-Al}_2\text{O}_3$  (A),  $\text{Mn1-Al1}$  (B), and  $\text{Mn-W-}\gamma\text{-Al}_2\text{O}_3$  (C) catalysts with  $p_{2\text{-CP}} = 0.001$  atm and oxygen excess (total flow rate 350 mL/min).

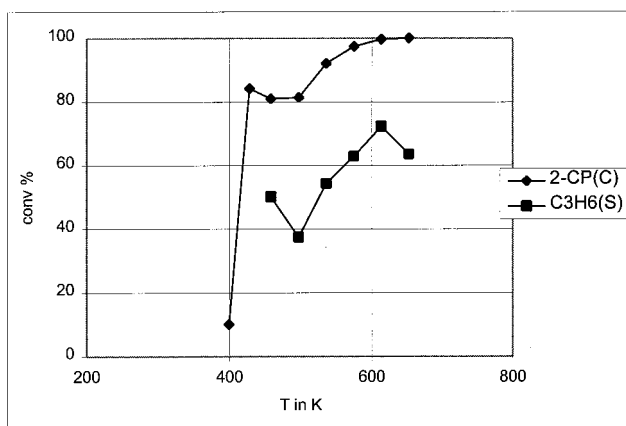


**Figure 6.** Conversion (C) of 2-CP and product selectivity (S) over ZSM5 catalyst with  $p_{2\text{-CP}} = 0.001$  atm and oxygen excess (total flow rate 350 mL/min).

**2.2. ZSM5 Catalyst.** 2-CP conversion has been studied also over a ZSM5 zeolite catalyst, thus a surface having Brønsted acidity. In this case 2-CP conversion starts above 400 K. Selectivity to propene follows a trend with a maximum (70%) at 580 K and then decreasing to 60% at 650 K (Figure 6). Several byproducts are

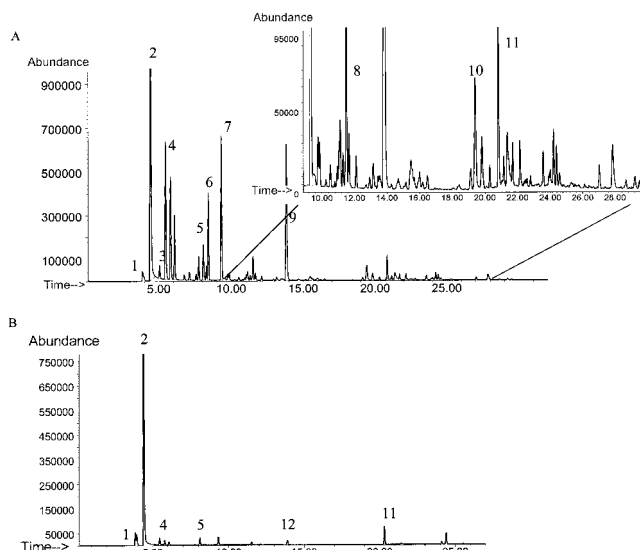


**Figure 7.** GC-MS analysis of the products arising from 2-CP conversion over ZSM5 catalyst at 548 K (A) and 673 K (B) with the same conditions as Figure 5: (1)  $\text{O}_2\text{-CO}_x$ , (2)  $\text{C}_3\text{H}_6$ , (3)  $\text{C}_4\text{H}_{10}$ , (4)  $\text{C}_4\text{H}_8$  isomers, (5)  $\text{C}_5\text{H}_{10}$  isomers, (6) iso- $\text{C}_3\text{H}_7\text{Cl}$ , (7)  $\text{C}_3\text{H}_5\text{Cl}$  isomers, (8)  $\text{C}_6\text{H}_{12}$  isomers, (9) dichloropropenes (i.e., 1,1-dichloropropene), (10)  $\text{C}_6\text{H}_{11}\text{Cl}$  and/or  $\text{C}_6\text{H}_{13}\text{Cl}$ , (11) toluene, (12)  $\text{C}_6\text{H}_6$ .

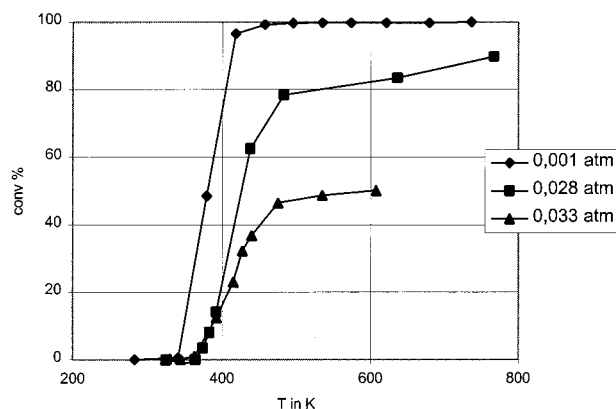


**Figure 8.** Conversions of 2-CP over 0.1 g of a  $\text{SiO}_2\text{-}\gamma\text{-Al}_2\text{O}_3$  catalyst at several 2-CP partial pressures. The total flow rate is the same for each catalytic run.

formed in significant amounts. It has been possible to identify most of them: isobutane and different butene isomers, unsaturated  $\text{C}_5\text{-C}_7$  hydrocarbons, including some cyclic compounds. The relative GC peak intensities (Figure 7) indicate the predominance of  $\text{C}_4$  (saturated and unsaturated) hydrocarbons and of pentenes and esene isomers in the temperature range between 540 and 600 K. Some chlorinated compounds are also formed, such as chlorinated  $\text{C}_4$  and  $\text{C}_5$  (i.e., chloromethylbutane and chlorobutane). At 623 K the amount of these compounds decreases, while cyclic and aromatic hydrocarbons, in particular cyclohexene, benzene, and toluene, resist at high temperatures, up to 740 K. At 600 K toluene is mainly formed together with higher molecular weight compounds.

After this run, the exhausted catalyst is completely black and an IR analysis has been performed. The spectrum of the catalyst in KBr shows typical bands of the zeolite structure and another sharp and strong band at  $1380\text{ cm}^{-1}$ , assigned to a CC stretching of a graphite-like material, indicating the formation of coke in the zeolitic cavities. These data allow us to conclude that ZSM5 zeolite is quite active in dechlorination of chlorine-



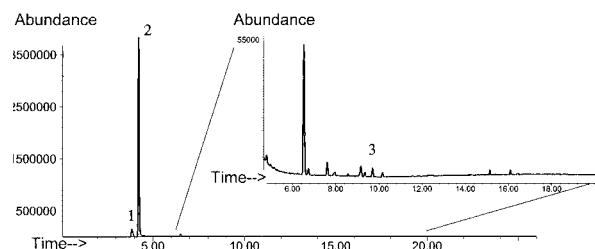


**Figure 9.** GC-MS analysis of the products arising from 2-CP conversion over a  $\text{SiO}_2\text{-}\gamma\text{-Al}_2\text{O}_3$  catalyst at 483 K ( $p_{2\text{-CP}} = 0.005$  atm, excess oxygen, total flow rate 350 mL/min): (1)  $\text{O}_2/\text{CO}_x$ , (2)  $\text{C}_3\text{H}_6$ , (3)  $\text{C}_3\text{H}_5\text{Cl}$  isomers.

containing organics (in fact, most of the products observed are hydrocarbons); however, it tends to coke so that deactivation is likely to occur.

**2.3. Silica-Alumina Catalysts.** In Figure 8 is shown the conversion of 2-CP on silica-alumina in the same conditions as for the previous experiments (0.001 atm of reactant). The conversion starts to be detectable near 320 K and is almost total near 450 K. Actually, the conversion curve in the range above 400 K is coincident with that calculated on the basis of thermodynamics, thus showing that, above this temperature, equilibrium is reached over this catalyst. Propene selectivity is also nearly total, and this is observed also with higher reactant concentrations. In Figure 9 a GC of a typical experiment performed with 0.005 atm of 2-CP is reported. The peak near 4 min of retention time is the propene product, that at 6 min is the residual 2-CP, and the main byproducts are chlorinated propenes (7–10 min), with their amount being lower than that of propene by a factor near 700. This makes this catalyst the best one among those we investigated here.

Considering its good dehydrochlorination activity and the almost total absence of chlorinated byproducts, this catalytic system has been the subject of a deeper investigation, carried out by varying the reaction conditions.

**3. Kinetic Evaluation over Silica-Alumina Catalysts.** **3.1. Effect of Contact Time.** In Figure 8 the conversion of increasing concentrations of 2-chloropropane over the same silica-alumina bed and the same total flow of the  $\text{He-O}_2\text{-2-CP}$  mixture has been investigated. Thus, the contact time is varied from  $\tau = 16.8 \text{ g}_{\text{CAT}}\cdot\text{s}/\text{mL}_{2\text{-CP}}$  (like in the above experiments) down to  $0.5 \text{ g}_{\text{CAT}}\cdot\text{s}/\text{mL}_{2\text{-CP}}$ . The conversion starts almost at the same temperature (near 370 K) in all cases except at the highest contact times (very diluted 2-CP concentration), where it starts a little earlier. The conversion curve has in all cases a rapid rise, but it is, at the higher starting partial pressures, well below that allowed by thermodynamics. Additionally, it later arrives nearly to a plateau. This plateau corresponds to total conversion only at the highest contact times, while in the other cases conversion is incomplete and tends to increase only slowly in the "plateau". The "plateau" is located at lower conversions the higher the 2-CP concentration. This behavior is typical of a two-range phenomenon where the kinetic regime is chemical in the strong conversion rise range and becomes external-diffusion-limited in the "plateau".<sup>22</sup>

Experiments at different contact times in the range  $\tau = 0.71\text{--}1.42 \text{ g}_{\text{CAT}}\cdot\text{s}/\text{mL}_{2\text{-CP}}$  have also been performed by varying the catalyst amount at the same flow conditions. The results are shown in Figure 10. It is evident that, within the experimental uncertainty,

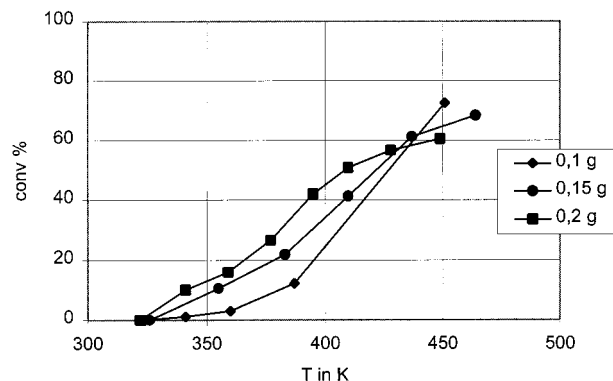


**Figure 10.** Conversions of 2-CP over 0.1/0.15/0.2 g of a  $\text{SiO}_2\text{-}\gamma\text{-Al}_2\text{O}_3$  catalyst with  $p_{2\text{-CP}} = 0.023$  atm. The total flow rate is 350 mL/min.

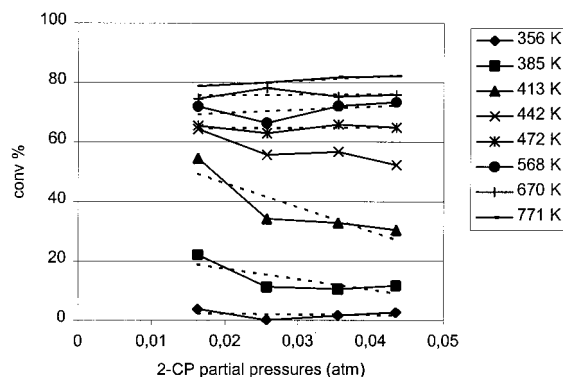


**Figure 11.** Conversions of 2-CP over  $\text{SiO}_2\text{-}\gamma\text{-Al}_2\text{O}_3$  catalyst at several 2-CP partial pressures fed and several reaction temperatures (same contact time  $\tau = 1.07 \pm 0.02 \text{ g}_{\text{CAT}}\cdot\text{s}/\text{mL}_{2\text{-CP}}$ ).

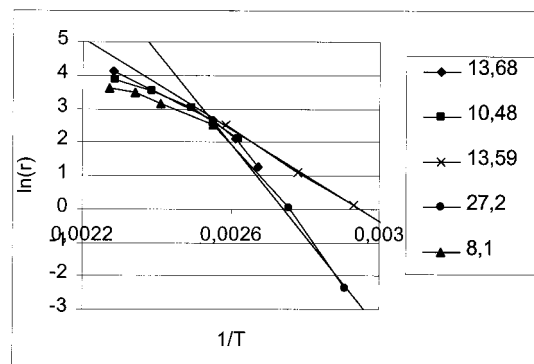


**Figure 12.** Arrhenius plot for several catalytic runs. The activation energies (kcal/mol) are reported in the right window.

below 410 K the conversion increases by increasing contact time, as expected. This agrees with a chemical kinetic regime below this temperature.

**3.2. Evaluation of the Reaction Order.** We can evaluate some kinetic parameters of our reaction assuming that the hypotheses for a differential reactor are fulfilled, so that we can assume the conversion as directly proportional to the reaction rate. In Figure 11 the conversions of 2-CP are plotted with respect to 2-CP concentration in experiments made with the same contact time ( $\tau = 1.07 \pm 0.02 \text{ g}_{\text{CAT}}\cdot\text{s}/\text{mL}_{2\text{-CP}}$ ). The amount of catalyst has, in fact, been varied in parallel to the variation of the 2-CP flow. It seems evident that 2-CP conversion in this range is substantially insensitive to its own concentration in the vapor phase or is slightly negatively affected, at least in the lower temperature-lower conversion range. This means that, in

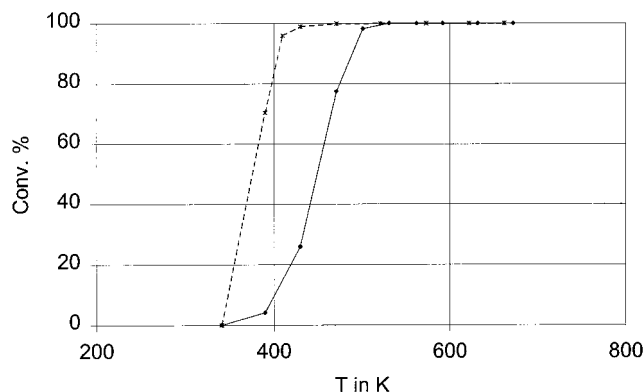


**Figure 13.** Conversion of 2-CP (dashed line) and of 1-CP (full line) over SCR catalyst with  $p_{2\text{-CP}} = 0.001$  atm and oxygen excess (total flow rate 350 mL/min).

**Table 2.** FT-IR Vibrational Mode for Liquid and Adsorbed 2-CP

assignment	liquid (ref 24)	Si-Al		Al <sub>2</sub> O <sub>3</sub>
		adsorbed at rt (this work)	adsorbed at 523 K (this work)	adsorbed at rt (this work)
$\nu(\text{asCH}_3)$	2986, 2975	2981		2973
$\nu(\text{sCH}_3)$	2931	2938		2937
$\nu(\text{CH})$	2915	2921 sh		2924
$2\delta(\text{CH}_3)$	2895	2899		
$\nu(\text{CH})$	2867	2874		2872
$\delta(\text{asCH}_3)$	1466	1467	1457	1466
$\delta(\text{CH}_3)$	1447	1450	1437	1449
$\delta(\text{sCH}_3)$	1386	1390	1406	1387
$\delta(\text{sCH}_3)$	1374	1376	1377	1375
$\delta(\text{CHCl})$	1260			1260
$\omega(\text{CH}_3)$	1161			1160
$\omega(\text{CC})$	1129			1131
				1107
$\omega(\text{CH}_3)$	1061			1061

these conditions and in the lower temperature range, the reaction order with respect to the reactant can be taken as zero or is a little negative.

**3.3. Evaluation of the Activation Energy.** In Figure 12 the Arrhenius plots of different experiments are reported. The data show that at low concentrations, where the assumption for the differential reactor can be taken as applicable, it is possible to measure (depending on the actual conditions of the experiments) an apparent activation energy of 27 kcal/mol (112.9 kJ/mol). At higher conversions where the assumption for

the differential reactor cannot be applied, we measure lower activation energies 8–15 kcal/mol (33.4–62.7 kJ/mol). These activation energies are sufficiently high and fall in the range of or are even higher than those already reported for dehydrochlorination processes over metal chlorides (30.4–91.3 kJ/mol).<sup>14</sup> On the other hand, the  $E_a$  measured at low temperature approaches those measured for the decomposition of secondary aliphatic alcohols on alumina.<sup>23</sup> This confirms that, at least in the low temperature–low conversion range, the kinetic regime is chemical. At higher conversions, a mixed regime can be reached.

**3.4. 2-CP versus 1-CP Conversion.** Over different catalysts, including SCR catalysts<sup>24</sup> and doped  $\text{WO}_3\text{--Al}_2\text{O}_3$ , we investigated the conversion of both 2-CP and its isomer 1-CP. Also 1-CP converts to propene and HCl, with a selectivity that approaches 100% in the best catalysts. This is shown in Figure 13 for a V–W–Ti oxide. 1-CP conversion is slower than 2-CP conversion over the same catalyst.

**4. FT-IR Studies over Alumina Catalysts.** 2-CP adsorption at room temperature gives rise to molecular weakly adsorbed species, characterized by IR bands at frequencies close to those of the liquid compound<sup>25</sup> (see Table 2). In the same spectrum, however (Figure 14), another weak but significant band can be detected at 1107  $\text{cm}^{-1}$ , which is not due to molecularly adsorbed 2-CP. In parallel, the OH stretching modes of the surface OH groups (3800–3600  $\text{cm}^{-1}$ ) disappear upon chloroalkane adsorption, causing the presence of negative peaks in the subtraction spectra. Interaction with 2-CP affects the different types of alumina surface hydroxy groups nearly in the same way.

Heating in the presence of the gas phase to 373–423 K gives rise to a completely different spectrum in the 1200–1000  $\text{cm}^{-1}$  region. The band at 1107  $\text{cm}^{-1}$  becomes predominant together with some other component at 1160, 1130, and 1061  $\text{cm}^{-1}$ . The CH deformation region shows almost the same bands as before at 1466, 1449, 1387, and 1375  $\text{cm}^{-1}$ , but the relative intensity changed and peaks at 1466 and 1387  $\text{cm}^{-1}$  become predominant. The band at 1260  $\text{cm}^{-1}$  is weakened. At 423 K the IR spectrum shows strong bands at 1200–1000  $\text{cm}^{-1}$  that can be ascribed to isopropoxy species<sup>26</sup> (CC/CO stretching modes) together with bands due to 2-CP, still molecularly adsorbed at the surface.

After further heating at 473 K, the overall spectrum changed again and correspondingly new adsorbed spe-

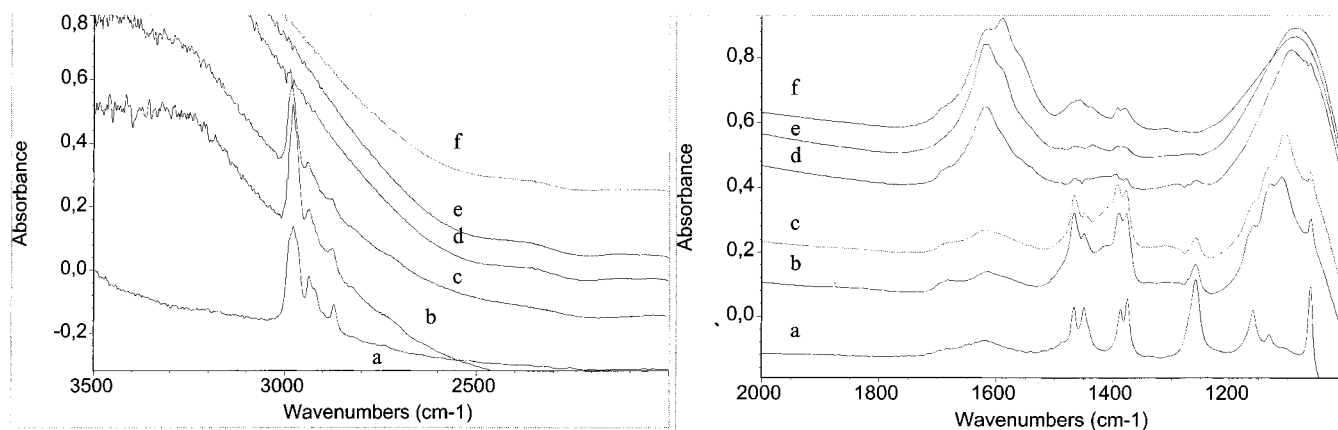


**Figure 14.** FT-IR spectra of the surface species arising from 2-CP adsorption over a  $\gamma\text{-Al}_2\text{O}_3$  surface in the presence of the gas: at room temperature (a), at 373 K (b), at 423 K (c), at 473 K (d), at 523 K (e), at 573 K (f). The activated surface and the gas-phase spectra have been subtracted.

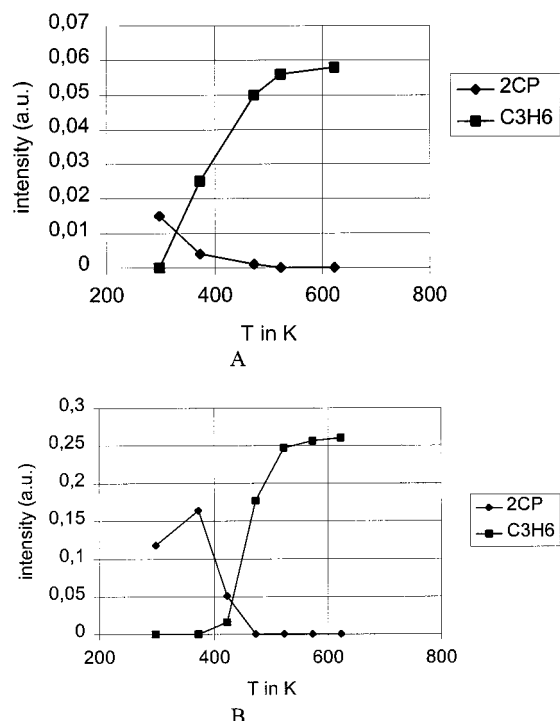


**Figure 15.** FT-IR band intensities of the gas-phase species detected during the 2-CP adsorption over  $\text{SiO}_2\text{-}\gamma\text{-Al}_2\text{O}_3$  (A) and the 2-CP adsorption over  $\gamma\text{-Al}_2\text{O}_3$  catalysts (B).

cies appeared. The bands in the CH stretching and deformation region weakened, showing that most of isopropoxide species and of adsorbed 2-CP disappeared. Bands at 1614, 1392, and  $1380\text{ cm}^{-1}$  are due to adsorbed formate species (COO asymmetric and symmetric stretching and CH deformation). At higher temperatures some more features appear at 1595, 1456, 1438, and  $1309\text{ cm}^{-1}$ , possibly assigned to other carboxylate species such as acetate or formate in a different coordination at the surface.

In the gas phase, propene formation (characterized by IR bands 912, 990, and  $1100\text{ cm}^{-1}$ ) starts to be detectable at 423 K (Figure 15 B) and propene is the only detected C-containing reaction product. HCl is also detectable in the gas phase starting from 423 K, following the presence of typical rotovibrational bands in the region  $2600\text{--}3000\text{ cm}^{-1}$ .

##### 5. FT-IR Studies over Silica–Alumina Catalysts.

Figure 16 shows the spectra arising from 2-CP adsorption over a silica–alumina surface at room temperature (a), after outgassing at room temperature (b), after heating in the presence of gas at 373 K (c), at 523 K (d), and at 623 K (e).

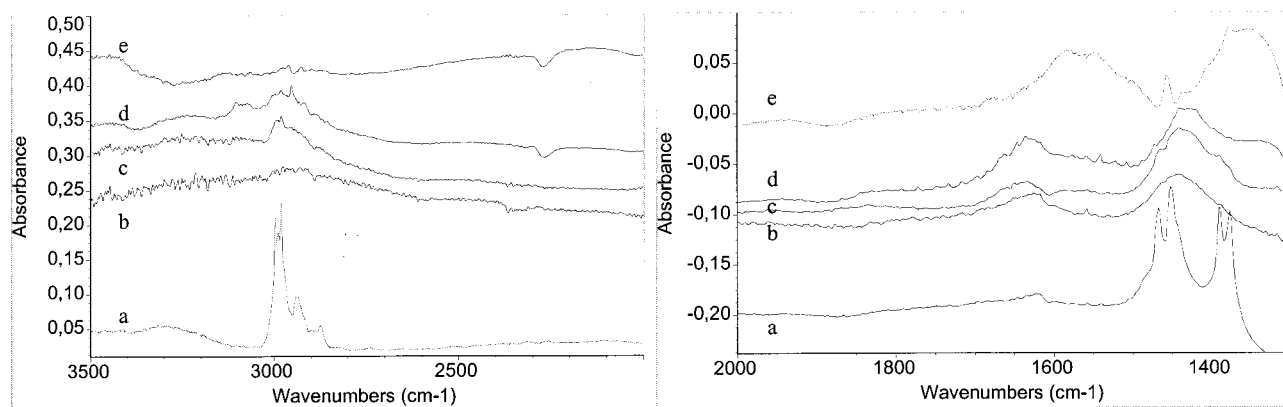


**Figure 16.** FT-IR spectra of the surface species arising from 2-CP adsorption over a  $\text{SiO}_2\text{-}\gamma\text{-Al}_2\text{O}_3$  surface at room temperature (a), after outgassing at room temperature (b), after heating in the presence of gas at 373 K (c), at 523 K (d), and at 623 K (e).

ing temperatures, in the presence of the gas phase. At room temperature the main bands in the spectrum centered at 1467, 1450, 1390, and  $1376\text{ cm}^{-1}$  are assigned to CH deformation modes of the  $\text{CH}_3\text{-CH-CH}_3$  group.<sup>27</sup> In the high-frequency region bands are detectable at 2981 (complex), 2938, 2921 (shoulder), 2899 (weak), and  $2874\text{ cm}^{-1}$  and are ascribed to CH stretching modes.

These bands are almost coincident with those reported in the literature for the liquid compound,<sup>25</sup> thus indicating a very weak interaction with the surface. In fact, these surface species disappear after outgassing at room temperature. Unfortunately the IR modes related with the CHX deformation and the CX stretching fall in the spectral region masked by the strong Si–O skeletal absorptions.

In the subtraction spectrum a negative feature centered at  $3745\text{ cm}^{-1}$  is observed, showing an interaction of the chlorocarbon with the terminal Si–OH groups that, however, does not disappear completely in the unsubtracted spectrum. It seems likely that at room temperature 2-CP interacts at least in part, giving rise to hydrogen bonds with the surface OH groups.

At increasing temperatures bands due to molecularly adsorbed 2-CP disappear, giving rise to strong and complex bands stable upon outgassing both in the region  $3000\text{--}2800\text{ cm}^{-1}$  and in the region  $1500\text{--}1300\text{ cm}^{-1}$ , with components at 1463, 1442, and  $1390\text{ cm}^{-1}$ . In this complex absorption components at positions similar to those observed for 2-propoxides on  $\text{Al}_2\text{O}_3$  are found. Both complex absorption modes disappear above 473 K. At higher temperatures bands due to residual carboxylate species can be detected.

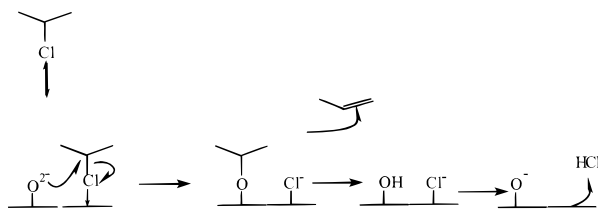
The spectra of the gas phase, recorded at increasing temperatures, show the formation of propene, already from 373 K. Between 523 and 573 K, 2-CP is totally converted to propene and HCl release in the gas phase can be detected only up to 523 K (Figure 15A).

##### Discussion

From the data presented above, it is evident that the acid catalysts studied reveal chloropropane dehydrochlorination activity.  $\text{WO}_3\text{-Al}_2\text{O}_3$  and silica–alumina appear to be, among the catalysts studied, those showing the lowest reaction threshold temperature ( $<400\text{ K}$ ). However, selectivities to propene differ significantly from catalyst to catalyst. This selectivity is low on the very acidic catalyst ZSM5 zeolite, according to the well-known ability of this material to promote oligomeriza-



Scheme 1



tion, cracking, and aromatization of hydrocarbon entities. The selectivity is also low in the case of the oxychlorination catalyst  $\text{CuCl}_2\text{--Al}_2\text{O}_3$  just because of its ability to insert chlorine which results in many deeply chlorided byproducts in agreement with literature data.<sup>28</sup> The selectivity over the other alumina-based materials is definitely better while silica–alumina is, among the catalysts used, the best in terms of selectivity, which always approached 100% in our experimental conditions. This actually agrees with the literature data where silica–alumina and silicates are reported to be used industrially for dehydrochlorination of higher chloroparaffins<sup>11–13</sup> and also of ethylene dichloride.<sup>7–9</sup>

The presence of oxygen in the reaction mixture allows part of the carbonaceous material that can be formed at the surface to burn, in agreement with the detection of very small amounts of CO and  $\text{CO}_2$  during the steady-state IR experiments. It has been observed that the catalyst, after 20 h of time on stream, is still active as the fresh catalyst, and an IR analysis does not reveal any adsorbed species. However, some carbonaceous material is present but easily burns in oxygen, giving rise to small amounts of  $\text{CO}_x$ . This suggests that the catalyst deactivates quite slowly and can be easily reactivated, if necessary.

The kinetic and mechanistic evaluation described above suggests that the reaction involves first a reversible adsorption step of 2-CP followed by an irreversible step involving a nucleophilic substitution of the chlorine atom by a surface catalyst oxide atom, giving rise to 2-isopropoxide species. These species later are eliminated, in the rate-determining step, to give propene and an OH group. Finally, HCl desorbs, restoring the surface oxide atom (Scheme 1). This mechanism arises from the IR spectroscopic data that show that the molecular adsorption of 2-CP is actually reversible while the adsorbed molecules evolves to alkoxide species which are more strongly adsorbed. Propene is found at higher temperature, and simultaneously alkoxide species disappear. HCl desorption is found relatively fast in the range 400–500 K. This picture seems to agree with the kinetic evaluation. The reaction order is zero or negative with respect to the reactant because of the saturation of the reactive sites by alkoxide species as a result of the low rate of the evolution of propene. The adsorption of HCl could also compete with the adsorption of the reactant, justifying a negative reaction order. The faster reaction rate of 2-CP with respect to 1-CP on the same catalysts with the same conditions suggests that the elimination step from the alkoxide to propene is actually rate determining, with a “monomolecular” E1 mechanism, i.e., through the formation of a carbenium ion. In fact, the formation of the secondary carbenium ion from 2-propoxide is expected to be faster than the formation of the primary carbenium ion from 1-propoxide. The activation energy we measured (near 15–30 kcal/mol) seems to be consistent with this reaction scheme, being likely associated with the heterolytic rupture of the

secondary C–O bond of the alkoxide species, as occurs for the decomposition of alcohols.<sup>23</sup>

## Conclusion

Silica–alumina is proposed as a good catalyst for the dehydrochlorination of 2-CP. The reaction occurs through the following steps: (1) reversible molecular adsorption; (2) nucleophilic substitution giving rise to 2-propoxide species; (3) elimination to propene; (4) desorption of HCl. The reaction occurs with a zero or slightly negative order kinetics and an activation energy in the range of 15–30 kcal/mol, which supports the idea that step 3 is rate determining and that sites for alkoxide formation can be saturated and HCl can have a competitive adsorption with the organic chloride. The rate of catalyst deactivation is apparently slow possibly because of the presence of oxygen in our reaction conditions.

## Acknowledgment

This research has been funded by the University of Genova.

## Literature Cited

- (1) Morrison, R. T.; Boyd, R. N. *Organic Chemistry*; Allyn and Bacon: Boston, 1985.
- (2) Chauvel, A.; Lefebvre, G. *Petrochemical Processes*; Ed. Technip: Paris, 1989; Vol. 1, pp 375–377.
- (3) Weissmermel, K.; Arpe, H. J. *Industrial Organic Chemistry*, 3rd ed.; VCH: Weinheim, Germany, 1997; p 122.
- (4) Jordan, J. I., Jr. *Chemical Processing Handbook*; McKetta, J. J., Ed.; Dekker: New York, 1993; p 357.
- (5) Weissmermel, K.; Arpe, H. J. *Industrial Organic Chemistry*, 3rd ed.; VCH: Weinheim, Germany, 1997; p 223.
- (6) Newmann, M. N. *Encycl. Polym. Sci. Eng.* **1985**, 17, 245.
- (7) Weissmermel, K.; Arpe, H. J. *Industrial Organic Chemistry*, 3rd ed.; VCH: Weinheim, Germany, 1997; p 219.
- (8) *Hydrocarbon Process.* **1999**, March, 148.
- (9) Dreher, E. L. *Ullmann's Encyclopedia of Industrial Chemistry*; VCH: Weinheim, Germany, 1986; Vol. A6, p 289.
- (10) Sotowa, C.; Watanabe, Y.; Yatsunami, S.; Korai, Y.; Mochida, I. Catalytic Dehydrochlorination of 1,2-Dichloroethane into Vinyl Chloride over Polyacrylonitrile-based Active Carbon Fiber. *Appl. Catal. A* **1999**, 180, 317.
- (11) Franck, H. G.; Stadelhofer, J. W. *Industrial Aromatic Chemistry*; Springer: Berlin, 1987; pp 211 and 212.
- (12) Chauvel, A.; Lefebvre, G. *Petrochemical Processes*; Ed. Technip: Paris, 1989; Vol. 1, p 192.
- (13) Weissmermel, K.; Arpe, H. J. *Industrial Organic Chemistry*, 3rd ed.; VCH: Weinheim, Germany, 1997; pp 79–80.
- (14) Ng, C. F.; Leung, K. S.; Chan, C. K. A Systematic Mechanistic Study of Dehydrochlorination of *tert*-Butyl Chloride on First Row Transition Metal Chlorides. *Proceedings of the 8th International Congress in Catalysis*, Berlin, 1984; DEHEMA: Berlin, 1984; Vol. III.
- (15) Ng, C. F.; Chan, C. K. Infrared Study of Dehydrochlorination of *tert*-Butyl Chloride on First Row Transition Metal Chlorides. *J. Catal.* **1984**, 89, 553.
- (16) Tavoularis, G.; Keane, M. A. Gas-Phase Catalytic Dehydrochlorination and Hydrodechlorination of Aliphatic and Aromatic Systems. *J. Mol. Catal. A* **1999**, 142, 187.
- (17) Tavoularis, G.; Keane, M. A. Direct Formation of Cyclohexene via the Gas-Phase Catalytic Dehydrochlorination of Cyclohexyl Halides. *Appl. Catal. A* **1999**, 182, 309.
- (18) Mochida, I.; Ukino, A.; Fujitsu, H.; Takeshita, K. Product Distribution in the Dehydrochlorination of Some Chloroalkanes over Alumina, Silica–alumina and Potassium hydroxide–Silica Gel. *J. Catal.* **1976**, 43, 264.
- (19) Finocchio, E.; Rossi, N.; Busca, G.; Padovan, M.; Leofanti, G.; Cremaschi, B.; Marsella, A.; Carmello, D. Characterization and Catalytic Activity of  $\text{CuCl}_2\text{--Al}_2\text{O}_3$  Ethylene Oxychlorination Catalysts. *J. Catal.* **1998**, 179, 606.



- (20) Carmello, D.; Finocchio, E.; Marsella, A.; Cremaschi, B.; Leofanti, G.; Padovan, M.; Busca, G. An FT-IR and reactor study of the dehydrochlorination activity of  $\text{CuCl}_2/\gamma\text{-Al}_2\text{O}_3$  based oxy-chlorination catalysts. *J. Catal.* **2000**, *191*, 354.
- (21) *Perry's Chemical Engineers' Handbook*, 7th ed.; Perry, R. H., Green, D. W., Eds.
- (22) Satterfield, C. H. *Heterogeneous Catalysis in Industrial Practice*; McGraw-Hill: New York, 1991; pp 483–485.
- (23) Pines, H.; Manassen, J. The mechanism of dehydration of alcohols over alumina catalysts. *Adv. Catal.* **1966**, *16*, 49.
- (24) Finocchio, E.; Baldi, M.; Busca, G.; Pistarino, C.; Romezzano, G.; Bregani, F.; Toledo, G. P. A Study of the Abatement of VOC over  $\text{V}_2\text{O}_5\text{--WO}_3\text{--TiO}_2$  and Alternative SCR Catalysts. *Catal. Today* **2000**, *59*, 261.
- (25) Klaboe, P. The Vibrational Spectra of 2-Chloro, 2-Bromo, 2-Iodo and 2-cyanopropane. *Spectrochim. Acta* **1970**, *26A*, 87.
- (26) Rossi, P. F.; Busca, G.; Lorenzelli, V.; Saur, O.; Lavalley, J. C. Microcalorimetric and FT-IR Spectroscopic Study of the Adsorption of Isopropyl Alcohol and Hexafluoro-isopropyl Alcohol on Titanium Dioxide. *Langmuir* **1987**, *3*, 52.
- (27) Lin-Vien, D.; Colthup, N. B.; Fateley, W. G.; Grasselli, J. G. *Infrared and Raman Characteristic Frequencies of Organic Molecules*; Academic Press: New York.
- (28) Lago, R. M.; Green, M. L. H.; Tsang, S. C.; Odlyha, M. Catalytic Decomposition of Chlorinated Organics in Air by Copper Chloride Based Catalysts. *Appl. Catal. B* **1996**, *8*, 107.

Received for review January 3, 2000  
 Revised manuscript received May 12, 2000  
 Accepted May 12, 2000

IE0000313